International Journal of Ocean Engineering and Technology Vol. 4, No. 1, pp 44~50, April 2001 (ISSN 1229-1668)

Characteristics of AE Signals from Fatigue Crack Propagation and Penetration of a Surface Crack in 6061 Aluminum Plate

SEOK-HWAN AHN AND KI-WOO NAM
Faculty of Engineering, Pukyong National University, Nam-gu, Pusan, 608-739, Korea
(Received 29 January 2001, accepted 2 April 2001)

ABSTRACT: *Existing surface defects in structural members often act as sites of fatigue crack initiation, and if undetected, these cracks may grow through the thickness of the member, leading to catastrophic failure of the structure. Thus, in-service monitoring of fatigue cracks through reliable and effective nondestructive techniques is an important ingredient in the leak-before-break (LBB) design and safe operation of defects critical structures. An advanced, waveform-based, acoustic emission (AE) technique has been used in this paper to study the characteristics of the signals emanating from the initiation, growth and through-the-thickness penetration of a surface fatigue crack in a 6061 aluminum plate. The goal of this experimental study is to determine whether the evolution of the fatigue cracks could be identified from the properties of the waveforms produced during the tests. The AE waveform signals detected at different stages of crack growth was found to have different temporal and spectral characteristics. The data analysis technique presented here can be applied to real-time monitoring of the initiation and propagation of fatigue cracks in structural components.*

KEY WORDS: Fail-safe design, Leak before break, Fatigue crack propagation, Penetration, Acoustic emission, Waveform, Power spectrum.

1. Introduction

The leak-before-break (LBB) design philosophy used for pressure vessels and energy-related plants (IMCO, 1975; Gilchrist, 1992) has been attracting much attention from the point of view of safety and economy. The LBB design aims to insure that content leakage will be detected before the component is subjected to catastrophic failure caused by unstable crack growth. In this sense, the LBB design can be considered as a fail-safe type design. However, the design requires that failure does not occur before cracks have propagated fully through the thickness, and that even after this event, unstable fracture does not occur for some fixed period of time. It is difficult to evaluate quantitatively the fatigue crack behavior after the penetration due to the fact that quantitative studies of fatigue crack propagation behavior under low fatigue stress, in three-dimensional, through-crack models are relatively few. Ando et al. (Ando, 1987) have proposed a simplified evaluation model for determining the stress intensity factor after penetration. They found that the crack propagation characteristics, the crack shape change, and the crack opening displacement in a variety of specimens could be evaluated using their model.

Acoustic emission monitoring is a very sensitive method with a wide dynamic range and can be used as diagnostics for continuous assessment of damage in materials and components (Nam, 1999; Nam, 2001; Nam, 2001). Methods based on acoustic emission can be applied to metallic (Takahashi, 1996) as well as composite structural components (Lim, 2000) subjected to static as well as fatigue loading (Liptai, 1971). In general, acoustic emission can be used to monitor crack initiation and propagation and to locate the source of the emission. Numerous studies have been conducted to determine the correlation between the characteristics of AE output and various fracture mechanics and fatigue damage parameters (Oh, 1998; Oh, 1999; Lee, 1999). It has been shown that under static loading AE can be used to detect yielding and that the cumulative AE output from a notched specimen is directly related to the stress intensity factor (Dunegan, 1969). Acoustic emission has been very useful in detecting crack initiation and propagation under fatigue loading (Fang, 1993; Kohn, 1992).

In this experimental study, the AE technique is applied to study the signal characteristics emanating from fatigue crack propagation and penetration in 6061 aluminum plates under fatigue loading (Nam, 1999). The AE waveforms generated during various stages of crack propagation and their power spectra are analyzed and classified (Nam, 2001). The waveforms generated during different stages of crack propagation are shown to have different specific characteristics that can be used to identify the evolution of fatigue cracks in structures through careful analysis of the waveforms captured by broadband sensors located in the structure.

2. Experimental Procedure

The material used in this study is 6061 aluminum; the specimen geometry and the initial notch configuration are shown in Fig. 1. The initial surface crack was made in an electric discharge machine (EDM). In all specimens the initial crack length $2a_0$ is 8.8(mm) and the crack depth b_0 is 2.4(mm).

The fatigue tests were performed at room temperature using a servo-hydraulic fatigue testing machine (INSTRON model 8501) under load control. The waveform was a sine wave with frequency 2Hz and the stress ratio(R) was 0.1. The applied load for both specimens was P = 15.7 kN. In both specimen, labeled AT1 and AT2, the test was carried out until fracture after surface crack (initial crack) penetrate the plate thickness. On the other hands, specimen AT2 only had retardation period after crack penetration.

The AE measurements were carried out using a Fracture Wave Detector (FWD) (Model F4000, Digital Wave Corp., Englewood, Co.). The FWD allows for the digitization of AE waveforms in real time. The digitization rate was set at 12.5 MHz with 1024 point gate length for each channel with a threshold of 0.2V. Two broadband transducers were placed at equal distances from the notch (see Fig. 1). Two 40dB preamplifiers (AET 140B) with 30kHz-2MHz plug-in filter were used in the experiments. As is well known, signal discrimination in presence of noise from a variety of sources is the most crucial problem in processing the AE data from the experiment. Background noise during testing can be hydraulic, electrical or mechanical. Various methods of noise suppression were studied and implemented. The grip sections of the specimens were covered with thin aluminum plates bonded by epoxy resin to reduce mechanical noise. Clay wrapped around the top and bottom sections of the specimen acted as additional damper for noise produced by the environment.

3. Fatigue Crack Propagation Behavior

A schematic diagram of the propagation behavior of the crack initiated at the notch is shown in Figure 2, based on similar studies carried out earlier in metallic specimens (Nam, 1993; Nam, 1994; Nam,1995). The trace of the crack on the front surface of the plate grows continuously with no significant effect from the propagation of the crack through the thickness of the plate and its penetration of the back surface.

The propagation characteristics of the crack on the back surface of the plate can be approximately classified into three stages as sketched in Fig. 2. Stage *"a"* applies to the period immediately after crack penetration through the plate thickness; where the trace of the crack grows at a rapid rate. During stage '*b*' the trace of the crack grows at an almost constant rate until it reaches a certain length. Finally, in stage 'c', the crack accelerates and the length of the crack trace on the back surface approaches that on the front surface. The AE events during crack propagation were categorized into four stages: *pre-penetration, a, b, c* and *retardation.*

The normalized cumulative counts are plotted versus normalized cycles for the two specimens, AT1 and AT2 in Fig. 3. In order to insure that the signals are from the crack or cracks initiated at the notch, only the signals detected at the two sensors at about same time were retained; the other signals are noise from various sources and were discarded. In both specimens the production of AE events was initially slow, but it increased rapidly as the crack approached the back surface and decreased just before penetration. The increase and decrease of the AE events as the crack approached the back surface can be attributed to the transition of the state of deformation from plane strain to plane stress conditions (Ando, 1985). This tendency was also observed in SS41 steel (Nam,1999).

In specimen AT1 the number of AE events increased rapidly with continued cyclic loading after crack penetration. In the stage '*retardation*' of specimen AT2, the emissions went down significantly just after load reduction. This is due to the fact that

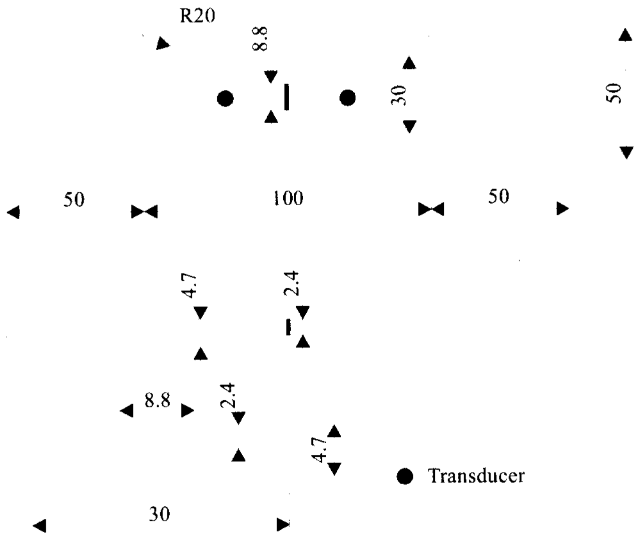

Fig. 1 Dimensions of specimens (unit : mm).

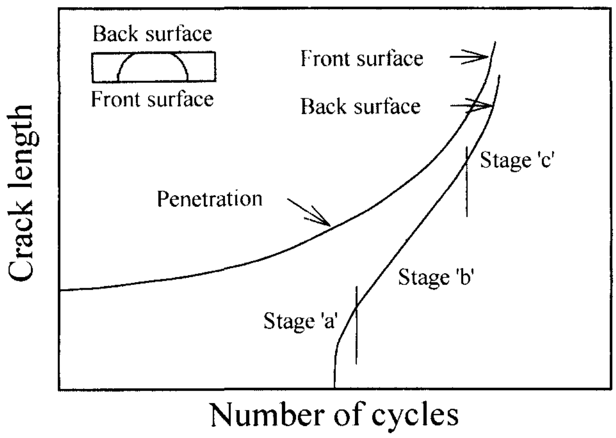

Fig. 2 Schematic diagram of crack propagation behavior in surface crack.

at the high load before load reduction, plastic deformation occurred near the crack tip and the residual plastic stress was relieved by subsequent cyclic loading (Elber, 1970).

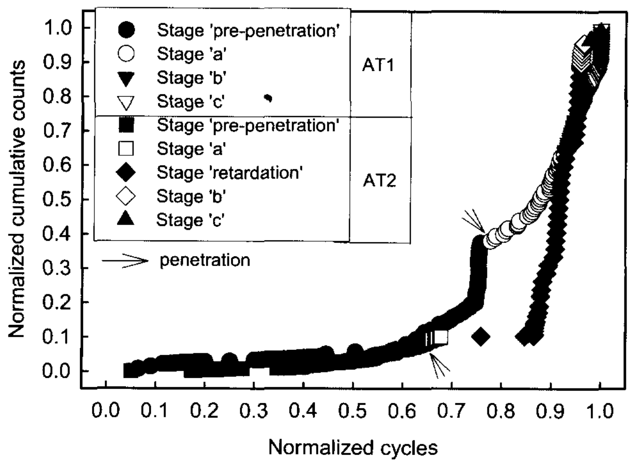

Fig. 3 Relationship between cumulative counts and load cycles.

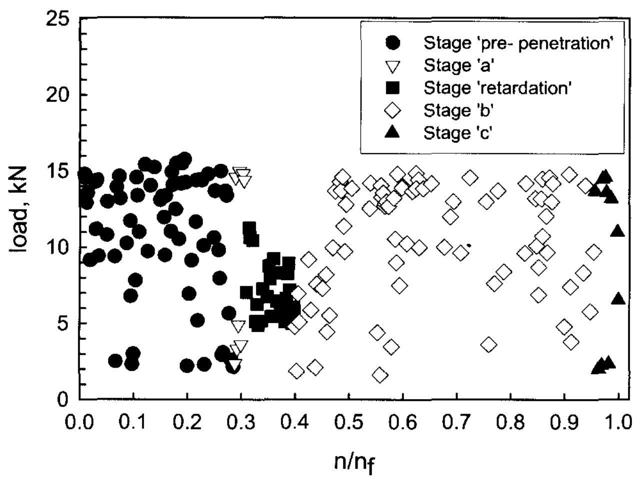

Fig. 4 Relationship between load and normalized acoustic emission at different stages of crack growth.

4. Signal Classification and Characterization

Since the surface trace of the initial crack (EDM notch) is larger than its depth (Fig. 1), the stress intensity factor at the bottom of the notch is larger than that at the edges of its surface trace. For specimen AT1 the initial stress intensity factor at the surface is approximately given by K_{as} = 9.95 MPa(m)$^{1/2}$ and at depth it is K_b = 11.26 MPa(m)$^{1/2}$. Therefore, the crack initiates first at the bottom of the notch and propagates more rapidly than its front surface trace. The front surface crack initiates and propagates afterwards, and eventually the crack penetrates the bottom surface of the plate.

A many signals were obtained during each stage of fatigue crack propagation. Fig. 4 shows the relationship between the load and the normalized acoustic emission number per stage for specimen AT2, where each symbol represents an AE event received by the sensors. Here n is the number of events for a given load and nf is the final number of events recorded for that load. Although many events took place at/ near the peak load over mean load, events also occurred when the load was near or at its minimum. In the *retardation* stage after load reduction, most of the AE events were produced by fretting of the fracture surfaces.

The AE signals were classified based on visual examination of their temporal and spectral features. The general procedure followed in the visual classification of the signals is sketched in Fig. 5. This resulted in the identification of six different types of signals, labeled Type-I~Type VI. In the power spectrum of each signal of Type-I has a dominant peak at approximately 0.5MHz, straddled by two smaller peaks. The power spectra of Type-II signals have a dominant peak at approximately 0.3MHz, and also few smaller peaks before and after the main peak. Type-III signals have a dominant peak at approximately 0.75MHz, and a small peak at a higher frequency. Type-IV signals have dominate peaks at approximately 0.3, 0.5 and 0.75MHz and also a peak before 0.3MHz and after 0.75MHz. Type-V signals have a

Table 1 Classification of AE events (%)

Specimen	Stage	Type I	Type II	Type III	Type IV	Type V	Type VI
	pre-penetration	42.9	-	6.1	51.0	-	-
	a	33.3	51.5	-	-	15.2	-
AT1	b	-	81.5	3.7	-	14.8	-
	c	90.0	-	-	-	10.0	-
	pre-penetration	41.7	-	7.4	51.9	-	-
	a	-	54.5	-	45.5	-	-
	b	-	72.2	-	-	17.8	-
AT2	retardation	-	4.0	-	-	-	96.0
	c	62.5	-	-	-	37.5	-

dominant peak at approximately 0.15MHz. Type-VI signals have a dominant peak at approximately 0.25 and 0.7MHz and a small peak at a higher frequency.

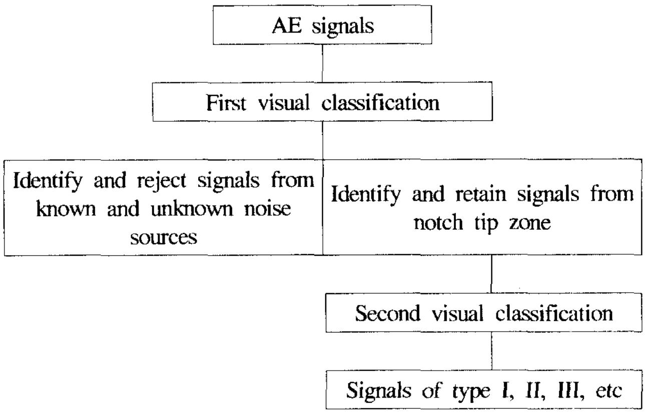

Fig. 5 Flow chart of the visual classification of AE signals.

Typical signals received from the five stages of crack propagation are presented in Fig. 6-10, and the relative number of the signal types from the different stages in the two specimens is shown in Table 1. It should be noted that the Type VI signals were obtained from the crack retardation stage in specimen AT2 only.

The waveforms and power spectra of the signals recorded in the pre-penetration stage are shown in Figure 6. The signals from this stage are of three types: Type-I, Type-III and Type-IV. The signals from Stage '*a*' are Type-I, Type-II and Type-V and are shown in Figure 7. The signals from stage '*b*' can be classified into Type-II, Type-III and Type-V, and are shown in Figure 8. The signals from Stage '*c*', in which the length of the crack trace are about the same on the front and back surfaces of the plate, can be classified into Type-I and Type-V, and are shown in Figure 9. The waveforms and power spectra of the signals obtained from the retardation stage in specimen AT2, just after

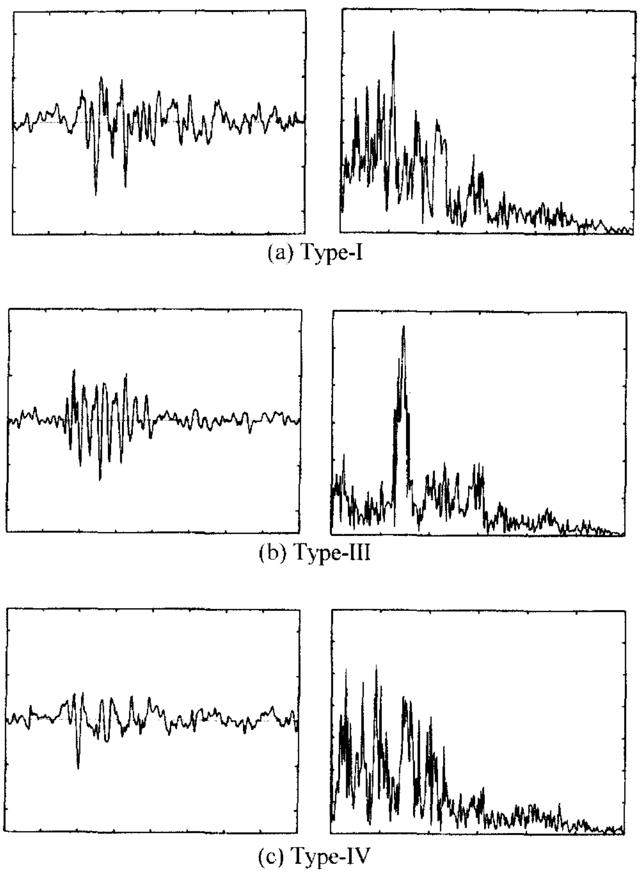

Fig. 6 AE events detected at the stage '*pre-penetration*' during fatigue crack propagation.
Horizontal scale: i) Waveform - 5(μs/div, ii) Power spectrum - 0.5MHz/div. Vertical scale is arbitrary.

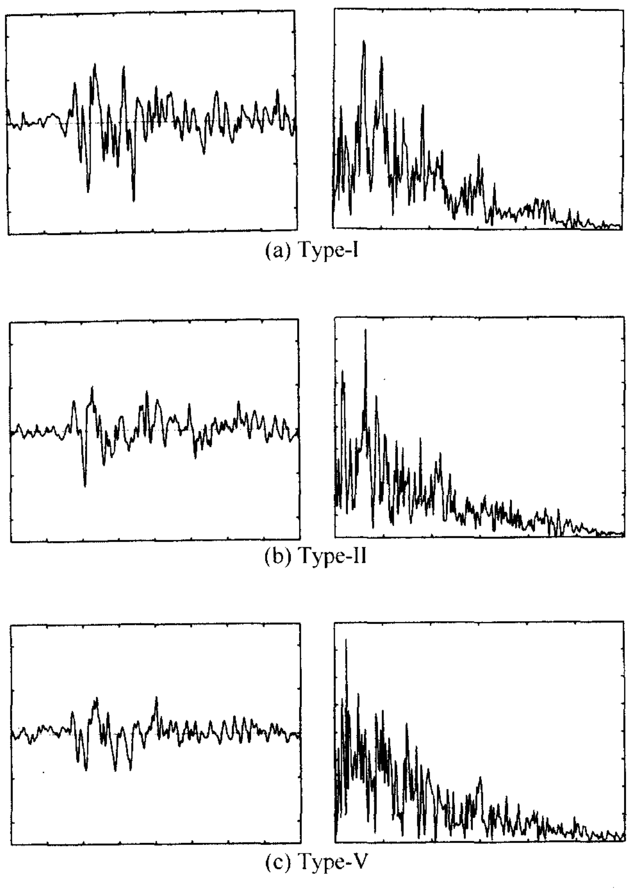

Fig. 7 AE events detected in stage '*a*', immediately after crack penetration through the back surface of the plate followed by rapid crack growth. Scales are the same as in Fig. 6.

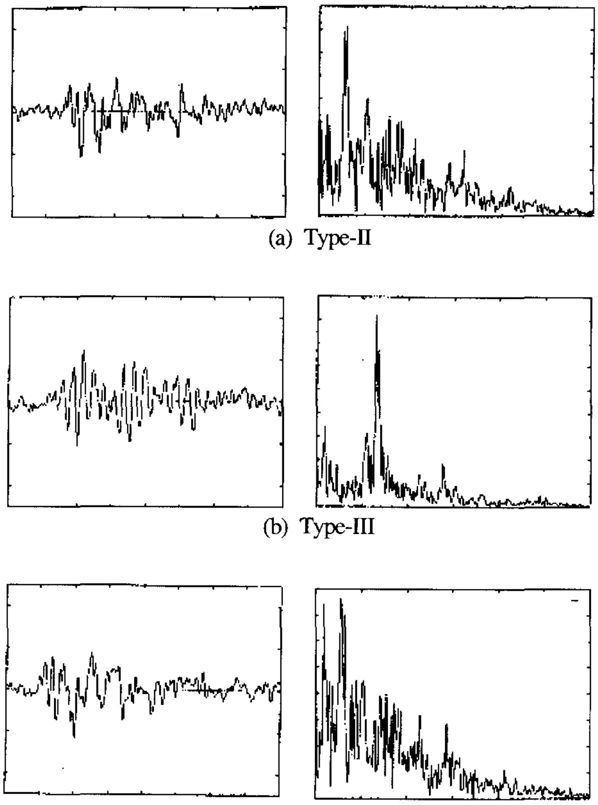

(a) Type-II

(b) Type-III

(c) Type-V

i) Waveform ii) Power spectrum

Fig. 8 AE events detected in stage 'b', during crack growth at nearly constant rate immediately after penetration. Scales are the same as in Fig. 6.

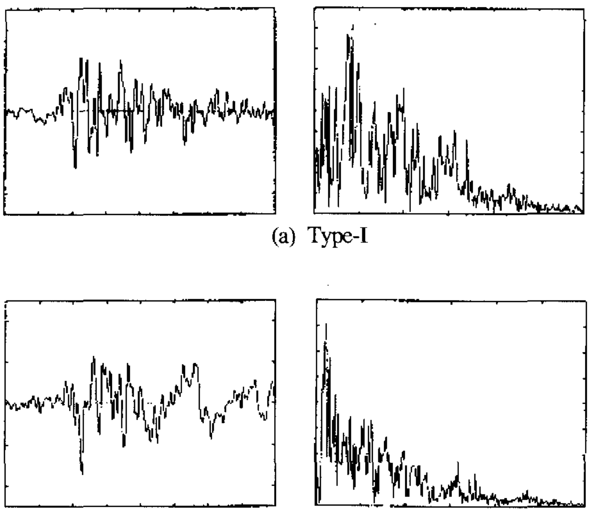

(a) Type-I

(b) Type-V

i) Waveform ii) Power spectrum

Fig. 9 AE events detected in stage '*c*' during accelerating crack growth in back surface of the plate. Scales are the same as in Fig. 6.

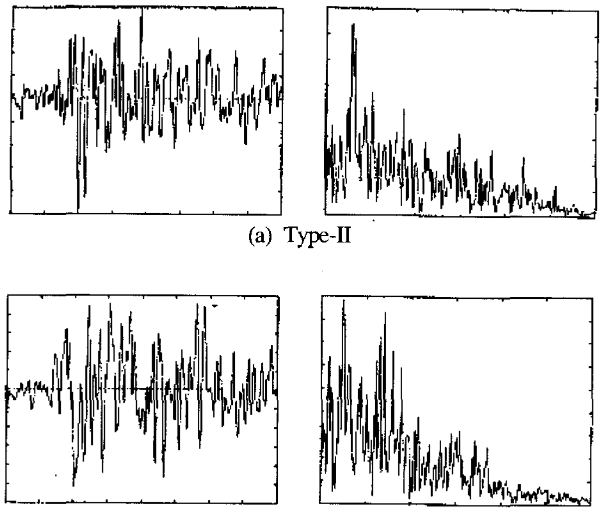

(a) Type-II

(b) Type-VI

i) Waveform ii) Power spectrum

Fig. 10 AE events detected during plastic unloading and stage '*retardation*' in crack grow. Scales are the same as in Fig. 6.

penetration are shown in Figure 10. These signals can be divided into Type-II and Type-VI. It can be seen that the main types of signals obtained in each stage for the two specimens are very similar although there are differences in some of their detailed features (see Table 1).

The waveforms of Type-IV signals obtained from the two specimens are characterized by a very sharp rise and decay and very short duration. These characteristics are typical of plate guided extensional and flexural waves(Guo, 1996). The stress ratio was changed from R = 0.1 to R = 0.42 in order to obtain the signals from fretting in the retardation stage after penetration in specimen AT2. The specimen displayed retardation behavior caused by varying the range of applied stress [19]. It displayed a large number of signals caused by fretting of the existing fracture surfaces. The waveforms of Type-II and Type-VI obtained from this stage were significantly longer duration than those observed in the other stages.

In the stage '*pre-penetration*', where the crack propagates in three-dimensions, the majority of the signals were Type-I and Type-IV. Stages '*a*' and '*b*', after penetration, produced mainly Type-II signals. On the other hand, 96% of the fretting signal by retardation behavior in stage '*b*', after penetration, were Type-VI. Final fracture, stage '*c*', had mainly signals of Type-I, but a little Type-V.

The AE signals detected during the five stages, namely, stage '*pre-penetration*', stage '*a*', stage '*b*', stage '*c*' and stage '*retardation*' were found to be different. Signals from the stage before penetration had a dominant peak at a relatively high frequency (0.5~0.75MHz), while those from stages '*a*' and '*b*', after penetration, had dominated peaks at a relatively low frequency of approximately 0.3MHz. The dominant frequency of the signals from stage '*c*' was at about 0.5MHz. Signals from the stage '*retardation*', after penetration, had dominated peaks at approximately 0.25 and 0.7MHz.

5. Conclusion

An advanced waveform-based acoustic emission (AE) techniques was applied to study the characteristics of the acoustic emission signals emanating from fatigue crack propagation and penetration in 6061 aluminum plates under fatigue loading. The waveforms and power spectra of the detected signals associated with the various stages of crack propagation were analyzed based on their spectral characteristics. It was found that the AE events increase significantly as the crack approached the back surface of the plate, and decreased just before it penetrated the back surface. Only a small number of AE events were observed during crack retardation and stress unloading after penetration; these were mainly due to fretting between the crack faces.

From the analysis of the waveforms and their power spectra for a 6061 aluminum plate containing a surface crack, it is possible to monitor, in real-time, the crack propagation and penetration behavior, along with damage and defects in structural members.

References

(1) Ando, K., Fujibayashi, S., Nam, K. W., Takahashi, M. and Ogura, N., "The Fatigue Life and Crack Through-Thickness Behavior of a Surface-Cracked Plate (for the Case of Tensile Load)," JSME Int. J., Vol. 30, pp 1898~1905, 1987.

(2) Ando, K., Matsushita, H., Fujibayashi, S. and Ogura, N., "Separation and Fracture Toughness of Controlled Rolled Steel," J. Society of Materials Science, Vol. 34, pp 388~393. (in Japanese), 1985.

(3) Dunegan, H. L. and Harris, D. O., "Acoustic Emission - A New Nondestructive Testing Tool," Ultrasonics, Vol. 7, pp 160~166, 1969.

(4) Elber, W., "Fatigue Crack Closure under Cyclic Tension," Engng. Fract. Mech., Vol. 2, pp 37~45, 1970.

(5) Fang D. and Berkovits, A., "Fatigue Damage Mechanisms on the Basis of Acoustic Emission Measurements," Novel Exper. Techniques in Fracture Mechanics, ed. by A. Shukla, AMD, Vol. 176, ASME, pp 213~235, 1993.

(6) Gilchrist, M. D., Chipalo, M. I. and Smith, R. A., "Shape Development of Surface Defects in Tension Fatigued Finite Thickness Plates," Int. J. Press. Piping, Vol. 49, pp 121~137, 1992.

(7) Guo, D., Mal, A. and Ono, K., "Wave Theory of Acoustic Emission in Composite Laminate," J. of Acoustic Emission, Vol.14, pp s19- s46, 1996.

(8) IMCO Resolution A 328(IX) "Code for the Construction and Equipment of Ships Carrying Liquefied Gases in Bulk", 1975.

(9) Kohn, D. H., Ducheyne, P. and Awerbuch, J., "Acoustic Emission during Fatigue of Ti-6Al-4V : Incipient Fatigue Crack Detection Limits and Generalized Data Analysis Methodology," J. of Materials Science, Vol. 27, pp 3133~3142, 1992.

(10) Lee, B. S., Oh, S. K. and Park, H. D., "Creep Life Prediction by ISM for Dissimilar Friction Welded Joints of Turbine Impeller Super Heat Resisting Steel and AE Evaluation (2) - FRW and AE Evaluation," Int. J. Ocean Engineering and Technology, Vol. 2, pp 35~40, 1999.

(11) Lim, J. K and Song, J. H., "Thermal Characteristic Evaluation of Functionally Graded Composites for PSZ/Metal," KSME International Journal, Vol. 14, pp 298~305, 2000.

(12) Liptai, R.G., Harris, D. O., Engle, R, B. and Tatro, C. A., "Acoustic Emission Techniques in Materials Research," Int. J. of Nondestructive Testing, Vol. 3, pp 215~275, 1971.

(13) Nam, K. W., Ando, K. and Ogura, N., "The Effect of Specimen Size on the Behaviour of Penetrating Fatigue Cracks," Fatigue Fract. Engng. Mater. Struct., Vol.16, pp 767~779, 1993.

(14) Nam, K. W., Ando, K., Ogura, N. and Matui, K., "Fatigue Life and Penetration Behaviour of a Surface Cracked Plate under Combined Tension and Bending," Fatigue Fract. Engng. Mater. Struct., Vol. 17, pp 873~882, 1994.

(15) Nam, K. W., Ando, K. and Ogura, N., "Surface Fatigue Crack Life and Penetration Behavior of Stress Concentration Specimen," Engng. Fract. Mech., Vol. 51, pp 161~166, 1995.

(16) Nam, Kiwoo, "Acoustic Emission from Surface Fatigue Cracks in SS41 Steel," Fatigue Fract. Engng. Mater. Struct., Vol. 22, No. 12, pp 1103~1109, 1999.

(17) Nam, K. W., Kim, S. J., Lee, K. C., Oh, J. H., Oh, S. K. and Lee, J. S., "Acoustic Emission during Fatigue Crack Penetration Behavior of Surface Cracked Plate." J. of Ocean Engineering and Technology, Vol. 11, pp. 29~38, 1997.

(18) Nam, K. W., Mal, A.K. and Wei, R.P., "Characteristics of Acoustic Waveforms generated by Fatigue Crack Extension from Corrosion Sites in Aluminum Alloys," Proc. Third FAA/DOD/NASA Conference on aging Aircraft, Sept 20-23, 1999, pp 299~306, 1999.

(19) Nam, K. W., "A signal Characteristics of the Acoustic Emissions from the Fatigue Crack Propagation in 2024 Aluminum with Rivet Hole." J. of Ocean Engineering and

Technology, (in press), 2001.

(20) Nam, K. W. and Kim, S. J., "Life Prediction by Retardation Behavior of Fatigue Crack and its Nondestructive Evaluation." J. of Ocean Engineering and Technology, Vol. 13, pp 36~48, 1999.

(21) Nam, K. and Lee. J., "Acoustic Emission from Fatigue Crack Extension in Corroded Aluminum Alloys." J. of the Korean Institute of Gas, Vol. 5, pp 1~6, 2001.

(22) Nam. K. and Mal, A., "Characteristics of elastic waves generated by crack initiation in aluminum alloys under fatigue loading.," Journal of Materials Research, Vol. 16, pp 1745~1751, 2001.

(23) Oh, S. K., "Effect of Initial AE Counts during Plastic Deformation in Friction Welding." Int. J. of Ocean Engineering and Technology, Vol. 1, pp 56~61, 1998.

(24) Oh, S. K., Park, H. D. and Lee, B. S., "Friction Weld Quality Evaluation of Hydraulic Valve Spool Material by Acoustic Emission Technique." Int. J. of Ocean Engineering and Technology, Vol. 2, pp 18~25, 1999.

(25) Takahashi, H., Lim, J. K. and Song, J. H., "Thermal Shock/Fatigue Evaluation of FGM by AE Technique," KSME International Journal, Vol. 10, pp. 435~442, 1996.

(26) Wheeler, O. E., "Spectrum loading and crack growth," J. of Basic Engng., Vol. 90, pp 181~186, 1972.